The mechanics of non-Euclidean plates†

Eran Sharon and Efi Efrati

Received 6th June 2010, Accepted 13th July 2010
DOI: 10.1039/c0sm00479k

Non-Euclidean plates are plates ("stacks" of identical surfaces) whose two-dimensional intrinsic geometry is not Euclidean, *i.e.* cannot be realized in a flat configuration. They can be generated *via* different mechanisms, such as plastic deformation, natural growth or differential swelling. In recent years there has been a concurrent theoretical and experimental progress in describing and fabricating non-Euclidean plates (NEP). In particular, an effective plate theory was derived and experimental methods for a controlled fabrication of responsive NEP were developed. In this paper we review theoretical and experimental works that focus on shape selection in NEP and provide an overview of this new field. We made an effort to focus on the governing principles, rather than on details and to relate the main observations to known mechanical behavior of ordinary plates. We also point out to open questions in the field and to its applicative potential.

1. Introduction

The capability of soft elastic materials to undergo large deformations leads to different types of mechanical instabilities that often break spatial symmetries, generate small or multi-scale structure and re-distribute stresses within the material. Such instabilities are usually induced by the application of external confining forces or geometries. The confinement results in the buildup of internal stresses, which may drive these instabilities. On the other hand, natural bodies that are made of soft tissue, such as flowers, skin, or leaves often undergo specific mechanical instabilities when they are free of external confinement. Can we engineer bodies to shape themselves into desired configurations without the need of external confinement?

Even unconstrained elastic bodies may contain stresses. These are termed *residual stresses*. These often appear as artifacts during the manufacturing of materials, when different parts of a body swell/shrink differentially. In most cases, one wishes to avoid these stresses, as they cause uncontrolled deformation of the body and may even lead to its failure. For example, glass blowers anneal their products in order to avoid fracture due to residual stresses. On the other hand if we could control this mechanism and design bodies with controllable distribution of residual stresses, it would be possible to harness these mechanical instabilities, turning them into a powerful design and shaping mechanism.

Two main problems prevent a breakthrough in this direction. First, there are great difficulties in formulating a practical theoretical model of these mechanisms. The large deformations and material displacement that are involved prevent, in general, a successful linearization of the problem. The definition of elementary mechanical and geometrical quantities on such bodies, turn out to be tricky. For example, residually stressed bodies do not have any stress-free configuration. It is then impossible to use the common definition of strain, which is based on a map between the (non-existing) stress-free and a given configuration. To overcome such a basic difficulty one needs to either use the notion of "virtual configurations" or to use a covariant formalism, in which strain is expressed by metric tensors, rather than by configurations. The reader can find

The Racah Institute of Physics, The Hebrew University of Jerusalem, Israel
† This paper is part of a *Soft Matter* themed issue on The Physics of Buckling. Guest editor: Alfred Crosby.

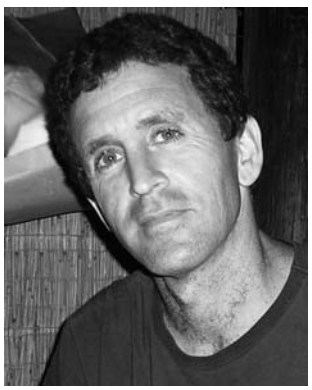

Eran Sharon

Eran Sharon is a professor of physics at The Hebrew University of Jerusalem. He is conducting experimental studies of different pattern forming systems. In particular, his research is focused on the mechanical instabilities in residually stressed bodies, mechanics of growth in plants, and instabilities in fluids under rotation.

Efi Efrati

Efi Efrati obtained his B.A. in maths and physics from the Hebrew university of Jerusalem, where he also pursued his M.A and Ph.D. (2010), both in nonlinear physics. His Ph.D. study was carried out under the guidance of Prof. Eran Sharon and Prof. Raz Kupferman and treated the elastic theory of non-Euclidean plates. He is currently a Simons post-doctoral fellow at the James Franck institute at the University of Chicago.

literature on both these approaches in works, staring in the 60's[1] through to the 90's and into the 21st century.[2–4] A second theoretical challenge would be to convert these formalisms into practical, easy to use *effective theories* that allow the deduction of general scaling laws, as well as predictions and efficient analysis of specific cases. Such effective theories, as well as computational tools designed to analyze these types of bodies, hardly exist.

Beyond the theoretical difficulties there is also a major problem of implementation. For example, assuming we know exactly what distribution of local shrinking and swelling will turn a disc of an elastic material into an ornamental bowl. How can we achieve it? How can we "program" the material to undergo different, known, local deformations at each point within it?

This paper focuses on an interesting kind of shape transforming, residually stressed soft bodies, in which concurrent theoretical and experimental progress were achieved. These are thin elastic plates that undergo lateral (in-plane) differential swelling/shrinkage; termed non-Euclidean plates. The physics of non-Euclidean plates is gradually being revealed, but there are still many open questions, as well as surprises, associated with their shape selection principles and their applicative potential. In this paper we will give an overview on this relatively new subject and will try to highlight potential directions for future progress, as well as open questions.

We start with a brief review on "ordinary" buckling and wrinkling instabilities trying to highlight the similarities and differences in their origins and characteristics. This will serve us later, when we discuss the mechanics of non-Euclidean plates (NEP). Next we show how to describe a local active lateral deformation (growth) using tools of differential geometry. Using these tools we write the energy functional of NEP and discuss its characteristics. In section 4 we describe the techniques that are available for building NEP, these include "homemade" NEP and advanced techniques that allow good control over the imposed "growth" and its external activation. Experimental and numerical results that highlight the underlying principles in shaping NEP are reviewed in section 5. We conclude in sections 6 and 7, mentioning potential applicative directions, central open questions and promising directions of progress in this field.

2. Mechanical instabilities of flat plates

2.1 Buckling

Buckling is a mechanical instability occurring in slender elastic bodies, which allows a reduction of in-plane compression by out of plane bending. We start by considering a ruler of length L and thickness t which is compressed by a given in-plane displacement 2δ of its edges (Fig. 1 top). If we assume the solution obeys the up-down symmetry of the problem, *i.e.* a flat configuration, we end up with energy density of a "compressed spring" $E_S \propto t\left(\frac{\delta}{L}\right)^2$ (Fig. 1 middle). We can consider a second solution, in which the system uses the three-dimensionality of the space in which it is located, breaks the up-down symmetry, and bends to form a perfect arc (Fig. 1 bottom). We can select an arc that perfectly obeys the boundary conditions while keeping the center-plane of the ruler (dashed line in Fig. 1) in its original length L. Estimating the energy of this configuration we note that "layers" of bottom

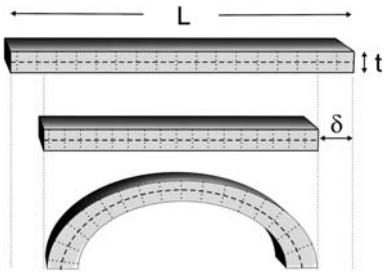

Fig. 1 Buckling of a ruler. A ruler of length L and thickness t is compressed by an amount 2δ (top). A pure stretching configuration (middle) is flat. In the pure bending configuration (bottom) the ruler is bent into an arc, while its mid plane (dashed line) preserves its length L. Within most plate theories approximations, lines that were perpendicular to the mid plane (dotted lines) remain perpendicular and preserve their length t.

parts of the ruler are compressed, while those on its upper part are stretched. For radius of curvature much larger than the sheet thickness it is plausible to assume[5] that material lines that were normal to the mid-plane at rest remain approximately normal in the bent configuration (dotted lines in Fig. 1). In this case the amount of stretching/compression of a "layer" is linear with its distance from the mid-plane. Squaring the strain (to get the energy density) and integrating over the thickness we find that the energy of the "pure bending" solution scales like $E_B \propto t^3k^2$, where k is the curvature of the ruler. The first, flat, solution we have constructed is called a pure stretching deformation. Its energy is linear with the thickness and square in the in-plane strain. The second type of solution is called a pure bending deformation. Its energy is cubic in the thickness and square in the curvature of the mid-plane.

If we gently compressed a thick ruler (very small δ, large t) it will stay flat. Now we start decreasing the thickness t. E_S will decrease linearly with t, but the energy of a pure bending configuration, E_B will decrease much faster, like t^3. There will be a thickness bellow which the pure bending deformation is energetically favorable, *i.e.* $E_B < E_S$. At this thickness it is clear that the pure stretching configuration is not the minimum of energy. Therefore the ruler will not stay in its flat configuration. Instead, it will buckle (up or down) into a curved shape. It is important to note that the actual configuration of the ruler will *not* be a pure bending one. It will still contain some stretching energy. For a thin enough ruler, the selected configuration will look very similar to a pure bending configuration. Still, it will have a lower bending energy and will contain some stretching (clearly we need to apply force on the rulers' edges to keep it buckled). The thinner the ruler is, the more expensive in-plane strains are compared to bending (the ruler becomes more floppy) thus the amount of in-plane strain decreases while the amount of bending deformations increases. As $t \to 0$, the configuration smoothly converges to the pure bending configuration, but never gets there. The full solution for this problem is beyond the scope of this paper and can be found in ref. 6.

2.2 Wrinkling

Let's consider the same ruler as before, however this time it is glued to a thick soft elastic substrate prior to its compression

(Fig. 2 top). This time, buckling of the ruler will deform the substrate, and will cost an additional energy E_{Sub} resulting primarily from the vertical stretching/compression of the substrate. When the ruler is much stiffer than the substrate and is sufficiently thin, it can be treated as non-stretchable. In this case the dominant energy terms are the bending energy of the ruler, E_B, and the substrate energy, E_{Sub}. The type of solution is set by the competition between the two, under the constraint that the ruler keeps its rest length L. For an oscillatory profile of amplitude A and wavelength λ, the ratio A/λ is constant for a fixed δ and L. The bending energy density scales like $t^3\lambda^{-2}$ and thus "prefers" the largest possible λ; a single arc configuration. However, as E_{Sub} increases with the vertical displacement of the ruler, it favors a configuration of vanishing amplitude. Due to the constraint on A/λ, such a configuration must have *vanishing* λ as well. One immediately notices that such vanishing wavelength configurations have diverging curvature, thus would cost *infinite bending* energy. Therefore, in this case, in contrast to buckling of the free ruler, one cannot construct a solution based on a "zero stretching configuration" to which the solution will smoothly converge. Instead, for every given thickness the full elastic problem must be solved by balancing the bending and stretching terms that favor large and small λ, respectively. The different dependence of each term on t (t^3 *versus* t^0 in this case) implies that λ has an explicit dependence on t and will approach zero in the limit $t \to 0$ (Fig. 2). This type of oscillatory configuration which refines as the thickness, t, decreases also appears in other scenarios.[7] The exact scaling with t depends on the thickness dependence of the competing energies. However, the approach to zero stretching *via* refinement of wavy solutions is quite general and is usually termed wrinkling (a detailed study can be found in ref. 7 and 8). A qualitatively similar behavior occurs without external compression, when the substrate shrinks much more than the skin.[9,10]

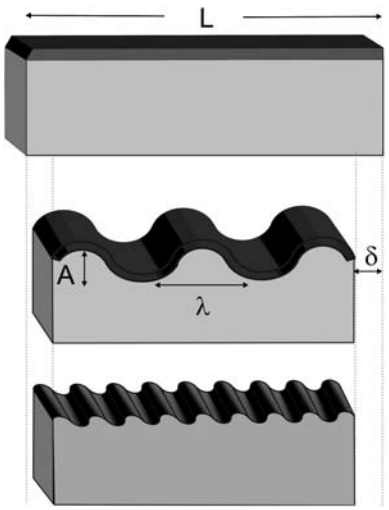

Fig. 2 Wrinkling. A stiff ruler of length L and thickness t is attached to a soft thick substrate. The system is compressed by an amount 2δ while the ruler keeps its original length L. For large thickness the bending stiffness of the ruler is large, leading to the selection of wavy surfaces with large wavelength and amplitude (middle). The thinner the ruler is, the floppier it becomes and the system selects wavy solutions of small wavelength and amplitude (bottom).

The above examples present two main types of deformations of thin plates (a third type—crumpling—will not be discussed in this paper). In both examples the mechanical instability is induced by the application of external compression on the, otherwise flat, body. In the next sections we will describe systems in which such instabilities occur in bodies that are free of external confinement. We will link the different configurations that appear, with either "ordinary buckling" or "wrinkling-like" instabilities.

3. Buckling and wrinkling of non-Euclidean plates

The classical example of buckling above shows how in-plane compression can lead to the formation of three-dimensional (3D) configurations. It is still difficult to see the connection to shaping of unconfined sheets, not subjected to any external compression or constraint. In the following section we show that when a plate swells (grows) laterally but non-uniformly it develops internal (residual) stresses that can lead to buckling or wrinkling-like instabilities even when the plates are free of constraints. We will present a formulation of the plate equation, which is efficient and "natural" for describing the problem.

Note that one dimensional differential growth does not result in residual stress (it simply leads to non uniform elongation of the body). Differential growth of a three dimensional body does lead to the buildup of residual stresses, yet these cannot be significantly reduced without compromising the integrity of the body. However, when one of the dimensions of the body is small, the body is effectively two dimensional. In such cases a large portion of the residual stress may be relaxed through the relative "energetically inexpensive" bending. This in turn will cause very small residual stress to manifest strongly and give rise to the convoluted shapes discussed here.

We start by considering a simple toy model (Fig. 3): take a thin disc of radius R and thickness t. Let all the material enclosed within a radius $\rho < R$ undergo a uniform isotropic growth by a factor η. What will the disc configuration be? Like in the (ruler) example in section 2.1 we can consider a flat configuration with no bending (Fig. 3 left). In this case the inner part of the disc will be compressed, both radially and azimuthally, while its outer part will be radially compressed and azymuthally stretched. Flat configurations are, thus, not stretch-free. The energy of all such configurations increases linearly with the thickness. The obvious question is whether we can find an analogue for the second type of configurations in section 2.1—a configuration that eliminates stretching by buckling out of plane into a pure bending configuration. In such a configuration (Fig. 3 right) the energy is expected to scale as t^3. Thus, also in this model, at small enough thickness it will be energetically preferable to spontaneously buckle out of plane. The example above suggests that *planar non-uniform growth of plates can lead to their buckling.*

3.1 The target metric, gauss theorem and non-Euclidean plates

In this section we define some geometrical concepts and their inter connections. These will serve us as the basic tools for characterizing and analyzing our plates. Every configuration of a sheet is associated with a metric g of its mid-surface. The metric includes all the information about distances between neighboring

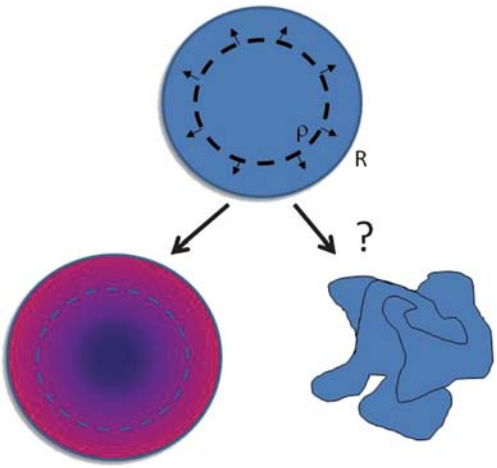

Fig. 3 Illustration of the construction and shaping of a residually stressed plate. Starting with an initially flat disc we let the material enclosed within radius r to undergo an isotropic growth in ratio η (top). The inner part of the disc is now too big to fit within the outer ring. Flat configurations of the disc will, thus, include in-plane stresses (bottom left). The colors illustrate the azimuthal stress: blue indicates compression, red indicates tension. If we can find a 3D configuration, which is free of in-plane strain, it would be a pure bending configuration (illustration on bottom right).

points on the mid-surface through $dl^2 = g_{ij}dx^i dx^j$. Every change of distances between points on the mid-surface will manifest as a change in the metric.

We begin, as before, with a stress-free flat elastic disc of radius R, thickness t and a polar coordinate system (r,θ). Using this coordinate system we can express the distance between two neighboring points,

$$dl^2 = dr^2 + r^2 d\theta^2,$$

which corresponds to the 2D metric tensor:

$$g = \begin{pmatrix} 1 & 0 \\ 0 & r^2 \end{pmatrix}.$$

Assume that somehow we induce a known position dependent planar growth of the material. Such a growth would *determine new equilibrium distances* between points on the mid-surface, distances for which each "spring" that connects neighboring points is at its rest length. We can define a new metric tensor—the "target metric", (as coined by Marder[11]), $\bar{g}$, which describes all these rest distances. When this body settles in a given configuration, it has a metric g, which can be different from $\bar{g}$. Whenever $g \neq \bar{g}$ there must be some "springs" that are not at their rest lengths. The material is, thus, strained. The local strain is simply the discrepancy between the metric of a given configuration, and the target metric at each point:

$$\varepsilon = \frac{1}{2}(g - \bar{g}) \tag{1}$$

This definition of strain is very natural to the problem: unlike the case of ordinary plates (such as the ruler), here we do not have a known stress-free configuration to start with. Only equilibrium *distances* between points are determined by the planar growth. This information is fully encoded in $\bar{g}$ and can be compared with the new distances as they appear in g. Note that we have no idea which sheet configuration, if any, obeys the target metric, but we know that if we find one, it will be free of in-plane strain.

Let's take a simple case: The induced growth of a disc is an axially symmetric azimuthal growth, which depends on the radius. Each element at radius r on the disc swells by a factor η(r) only in the azimuthal direction. The equilibrium distance between points is now:

$$dl^2 = dr^2 + \eta(r)^2 r^2 d\theta^2$$

And the target metric is:

$$\bar{g} = \begin{pmatrix} 1 & 0 \\ 0 & \eta^2(r) r^2 \end{pmatrix} \tag{2}$$

It expresses the fact that in order to obey the new equilibrium distances, the perimeter of a circle of radius r on the disc is no longer 2πr, but 2πη(r)r. For non-constant η this cannot hold when the sheet is flat. It must take a non-flat configuration.

3.2 The connection between metric and shape

A configuration of a sheet is represented by its mid surface (dashed line in Fig. 1). The shape of this 2D surface is characterized by the size and orientation of the local principle curvatures κ_1 and κ_2 at each point. The local mean and Gaussian curvatures are defined by $H = \frac{1}{2}(\kappa_1 + \kappa_2)$ and $K = \kappa_1\kappa_2$ respectively (see ref. 12). What can be said about configurations that obey a given metric g? This question is not new and was already addressed by Gauss who formulated his "Thorema Egregium", which is a key to understanding the mechanics of our plates. The theorem shows how the local metric coefficients (and their derivatives) fully determine the local Gaussian curvature on a surface (see ref. 12). In the context of the present problem Gauss theorem connects between growth and characteristics of the shape; growth specifies only distances that are expressed by a metric. However, according to Gauss it completely determines a Gaussian curvature at each point. A metric is flat (or Euclidean) if the Gaussian curvature associated with it is zero at every point. A metric is elliptic if K > 0 throughout the sheet and hyperbolic for K < 0. Specifically, the Gaussian curvature associated with a metric of the form

$$g = \begin{pmatrix} 1 & 0 \\ 0 & \varphi(x)^2 \end{pmatrix}$$

is simply

$$K = -\frac{1}{\varphi}\frac{\partial^2 \varphi}{\partial x^2} \tag{3}$$

Considering the physical sheet in the example above, we can calculate the "target Gaussian curvature" $\bar{K}$, which is determined by $\bar{g}$. $\bar{K}$ is an intrinsic property of the plate and should not be confused with the actual Gaussian curvature of the mid surface

K, which can be different from $\bar{K}$.) The target Gaussian curvature of the target metric in eqn (2) (where we have $\varphi = \eta r$) is:

$$\bar{K} = -\frac{1}{\eta r}\frac{\partial^2(\eta r)}{\partial r^2}$$

Some remarks on the Gaussian curvature:

In 2D the Gaussian curvature, K, is the only invariant of the metric and contains all the information about the local "shape" which is imposed by the in-plane growth.

If we use a different coordinate system, the metric might look very different, but K will be the same at every point. For example, the Gaussian curvature determined by the metrics:

$$g_{xy} = \begin{pmatrix} 1 & 0 \\ 0 & 1 \end{pmatrix}$$

And

$$g_{r\theta} = \begin{pmatrix} 1 & 0 \\ 0 & r^2 \end{pmatrix}$$

is zero. Indeed, the two metrics are those of a plane, the first in Cartesian and the second in polar coordinates.

We also notice that many different growth profiles can specify the same $\bar{K}$. They are thus geometrically equivalent. On the other hand eqn (3) is far from determining the shape of a surface. There is still a lot of freedom in selecting the principle curvatures and their directions. Thus, in general there will be many different surfaces having the same Gaussian curvature.

Having a plate with a given $\bar{K}$ (set by planar growth) we know that any of its stretch-free configurations must have Gaussian curvature K that is equal to the target one at every point. These are isometric *embeddings* of $\bar{g}$; realizations of the 2D metric as a surface in 3D. If the growth is such that $\bar{K} \neq 0$, these configurations cannot be flat. Instead, they will be curved 3D configurations.

The discussion above was focused on the 2D geometry of the bodies we consider. Despite their non-Euclidean planar geometry, our discs are plates—they are of finite thickness t and are "constructed" of *identical* surfaces stacked together from $-t/2$ to $t/2$. Thus, bending-wise they are identical to ordinary (flat) plates, having bending energy which increases with the local curvatures and vanishes only when they are flat. We have therefore suggested the name "non-Euclidean plates" for such bodies.[13]

3.3 Elastic energy functional

We are interested in the shape (equilibrium configurations) of NEP. These shapes will be minima of the elastic energy of the plate. We now present an approximate elastic energy functional for non-Euclidean plates: it is similar in spirit to the energy functional of ordinary (Euclidean) plates, being composed of a sum of a stretching term and a bending term.

$$E = E_s + E_b \tag{4}$$

Where the two energy terms are given by

$$E_b = \frac{Y}{24(1-\nu^2)}t^3 B, \quad E_s = \frac{Y}{2(1-\nu^2)}tS.$$

The stretching content, S, is a quadratic form of the metric discrepancy $(g - \bar{g})$, as given in eqn (1):

$$S = \int((1-\nu)\varepsilon^i_j\varepsilon^j_i + \nu\varepsilon^i_i\varepsilon^j_j)\mathrm{ds}$$

The bending content, B, is a quadratic form in the principle curvatures: $B = \int(4H^2 - 2(1-\nu)K)\mathrm{ds}$.

The later is identical to the bending content in Koiter's plate theory.[14] The stretching content, however, measures the discrepancy with respect to a not necessarily flat metric $\bar{g}$. In the case of ordinary (Euclidean) plates, the formalism recovers the Koiter plate theory.[14] With the addition of the small slope approximation it recovers the Foppl–Von Karman theory (see ref. 6).

A similar energy functional was assumed in early works on NEP[15,16] but only later was derived rigorously, starting from the full 3D elasticity theory.[13] Accurate definitions and expressions, including the derivation of equations of force and torque balance and an important discussion on non-Euclidean plates as 3D bodies can be found in ref. 13. An alternative energy functional for NEP in the Foppl–Von Karman limit was developed in ref. 17.

The bending and stretching terms in eqn (4) have to be evaluated with respect to two different "entities": the bending is measured with respect to a flat configuration, while the stretching with respect to a non-flat metric. This is required since the plate is *residually stressed* and does not have any stress-free configuration. Zero bending energy is obtained only at flat configurations. These do not obey the target metric, thus must contain stretching energy. Zero stretching is obtained at embeddings of $\bar{g}$, however, these must have $K(x,y) = \bar{K}(x,y) \neq 0$, thus have non-zero bending energy.

Similarly to other plate theories, the thickness sets the ratio between the bending and stretching rigidity. As the thickness decreases, stretching becomes energetically more expensive compared to bending. We thus expect that in the limit $t \to 0$ the sheets will adopt configurations with nearly zero stretching.

3.4 The $t \to 0$ limit

When searching for the equilibrium configurations of the physical sheets, we may start by considering the thin sheet limit and look for stretch-free configurations—configurations that fully obey the target metric. These are embeddings of $\bar{g}$ in space.

In general there are many isometric embeddings for a given metric and topology[12] and we need to select one. It was recently proven[30] that if there exists an isometric embedding of $\bar{g}$ with finite bending content then as $t \to 0$ the configurations of the physical plate converge to *the embedding of least bending content*. Such an observation is useful since minimizing bending content among embeddings of $\bar{g}$ could be a simpler task than minimizing energy among all possible configurations. It is not clear, however, what happens if there are *no isometric embeddings* for $\bar{g}$ with finite bending content.

To summarize this section we note that the energy functional of non-Euclidean plates has two terms: the stretching term which favors isometric embeddings of $\bar{g}$, and the bending term, which favors flat configurations. There is a competition between the

two terms which leads to shape selection. The energetic cost of bending, compared to stretching, decreases rapidly with the thickness. Therefore, the amount of in-plane strain decreases with thickness and the behavior in the vanishing thickness limit strongly depends on the nature of available embeddings of $\bar{g}$. In this sense there is an analogy between shape selection in free NEP and in confined flat sheets described in section 2. In the case of NEP the Euclidean space itself is the confining entity. In some cases this confinement is easily resolved; there exists low bending embeddings of $\bar{g}$ and at small enough thickness the plates settle in their vicinity, as in ordinary buckling. We might suspect that for some target metrics and topologies the confinement by space is such that all embeddings of $\bar{g}$ have high bending content. In this case the embeddings of $\bar{g}$ are not good candidates for minimization of the total energy at finite thickness and we expect to find a "wrinkling-like" behavior in some range of thickness. If all embeddings of $\bar{g}$ have infinite bending content the wrinkling-like behavior may persist all the way to the $t \to 0$ limit.

4. Building non-Euclidean plates

After presenting non-Euclidean plates and discussing their energy functional we turn to see if and how one can build such bodies. The idea is clear: take a thin elastic plate and change its target metric in a controlled way. Alternatively, directly build a non-Euclidean plate. Several techniques will be reviewed, while experimental and numerical results will be discussed in section 5.

4.1 Homemade NEP

Early experimental studies of NEP used plastic deformation as a mechanism for generating a non-Euclidean target metric. These experiments[18,19] were performed by a controlled tearing of a plastic sheet. The high stresses around the crack tip caused an irreversible plastic deformation of the initially flat sheet (Fig. 4). The plastic deformations, which determine the target metric $\bar{g}$, were measured. They consisted of elongation (increase in length) parallel to the tear edge (x direction) and were invariant along the crack propagation direction (x). The elongation was large close to the newly formed edge and decayed as some function φ of the distance from the edge, y. For this scenario the target metric can be written as:

$$\bar{g} = \begin{pmatrix} \varphi(y)^2 & 0 \\ 0 & 1 \end{pmatrix} \qquad (5)$$

The function $\varphi(y)$ was found to steepen towards the edge, having a positive second derivative. Thus, according to eqn (3), the tearing process resulted in $\bar{K} < 0$ which is invariant in the x direction. In these experiments we were able to modify the form of $\varphi(y)$ (although not substantially) by varying the material as well as the tearing velocity. However, there was no way to achieve good control over the metric, *i.e.* prescribe a specific $\varphi(y)$.

A demonstration of building a non-Euclidean plate from a flat plastic sheet is given in Fig. 5. In this figure, a polyethylene strip is uniaxially stretched (in the y direction). Due to necking instability, the plastic deformation, which is in-plane, is concentrated within a limited region in the strip. It consists of shrinkage in the x direction, dependent only on the y coordinate (Fig. 5 b). This, again, results in a new target metric which, after normalization (re-parameterization) of the y coordinate, is of the form of eqn (5). Note that the functional form of φ is qualitatively different from that of the tearing experiment. The target metric defines regions of positive, negative and zero Gaussian curvature. The free strip (Fig. 5 d) selects a 3D configuration, close to a body of revolution, consistent with its target metric.

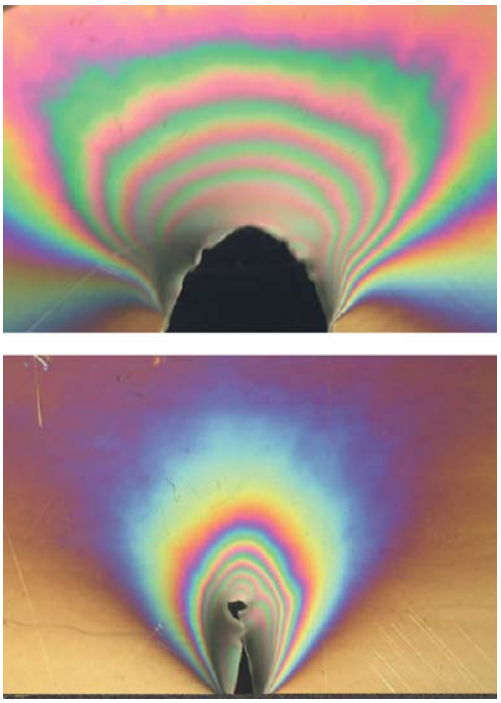

Fig. 4 Plastic flow generates a non-Euclidean target metric. Visualization of the deformation around the tearing tip, using photoelasticity. The density of isochromatic lines indicates the increase of deformation towards the tip. In the loaded state (top) the deformation field extends to large distances. When the sheet is unloaded (bottom) the deformation away from the tip, which is purely elastic, vanishes. However close to the crack tip there is a region which underwent an irreversible deformation. This deformation generated a new, non-Euclidean target metric.

"Homemade" NEP can be produced by crocheting. Controlling the number of stitches in a row is a direct way of determining a target metric. The earliest example the authors are aware of was given by Taimina[20] who "crocheted the hyperbolic plane". Crocheting curved sheets has recently became a popular hobby and the reader can find beautiful crocheted "coral reefs" and "flowers" in ref. 21 and http://crochetcoralreef.org.

4.2 Responsive NEP

A new technique of building NEP uses environmentally responsive gels.[22,23] These gels undergo reversible swelling/shrinking transitions that are induced by external fields. Gels that respond to various inducing fields, such as temperature[24] or concentration chemical agents,[25] are available and the response of the gel to the field can be sharp, "on-off-like", or gradual "analog-like". In previous work, we used NIPA gels which undergo a sharp shrinking transition above $C^{0}33$. We have found that the amount of shrinkage in the warm state is a strong function of the monomer concentration in the gel: gels with low monomer concentration lose up to 60% of their length at high

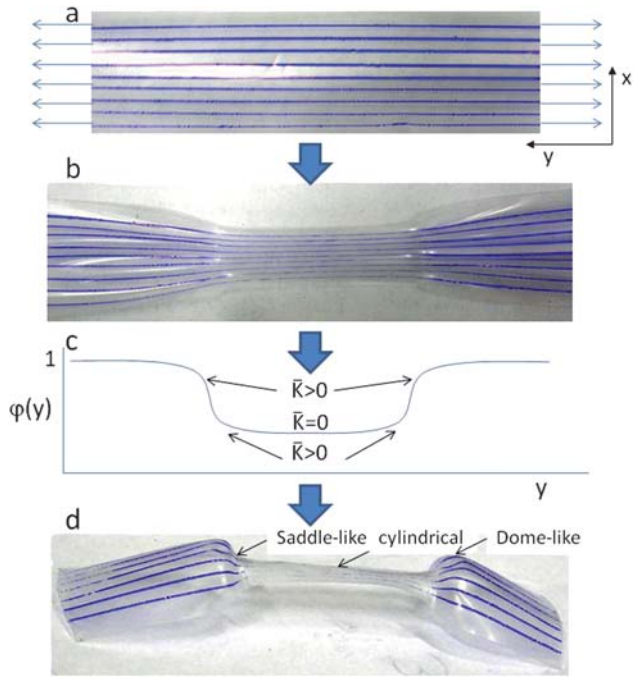

Fig. 5 (a) A Polyethylene strip is pulled horizontally in the y direction. (b) A necking instability leads to localization of the plastic deformation within a limited region. The equally spaced blue lines assist in visualizing the deformation field, which is invariant in the x direction. (c) A schematic of the function $\varphi(y)$ imposed by the plastic deformation. Arrows mark convex/concave regions of $\varphi(y)$, that are associated with negative/positive Gaussian curvature according to eqn (3). (d) The sheet, free of constraints, attains a 3D shape consistent with its target metric: The shape is approximately a body of revolution, with regions which are cylindrical, saddle-like (hyperbolic), and dome-like (elliptical). These correspond to the signs of $\bar{K}$ of (c).

temperature, while concentrated gels shrink by less than 10% of their length (Fig. 6).

Gel discs were made by injecting the NIPA solution, through a center hole, into a gap between closely spaced glass plates. The solution polymerizes within minutes forming an elastic thin plate. Non-Euclidean plates are made by a *controlled variation of the monomer concentration*, C, during injection. As the flow field is symmetric, we end up with a disc in which C = C(r). Such discs are flat when they are cold, but they are "programmed" to shrink by a different ratio at each radius. This differential "growth" by the shrinking ratio $\eta = \eta(r) = \eta(C(r))$, prescribes a new target metric (in polar coordinates) of the form:

$$\bar{g} = \begin{pmatrix} \eta^2 & 0 \\ 0 & r^2\eta^2 \end{pmatrix}. \qquad (6)$$

Introducing the arc-length radial coordinate on the shrunk disc ρ,

$$\rho(r) = \int_0^r \eta(r')dr',$$

transforms the target metric in eqn (6) to the form of eqn (2) (with respect to the new coordinate).

Thus we can use the concentration profile as a knob, with which we can prescribe $\bar{K}(\rho)$ on the disc. Examples of different

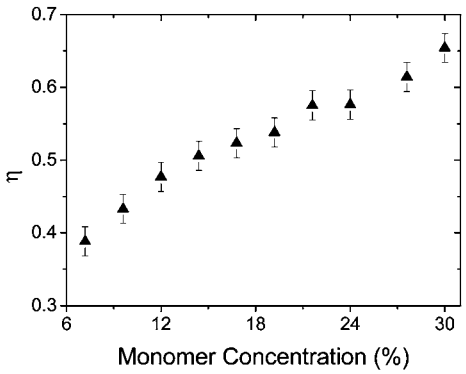

Fig. 6 The shrinking in length of a NIPA gel as a function of the monomer concentration. Gel discs of uniform concentration were equilibrated in a warm bath for 24 h. η is the ratio between the diameter of a warm disc and the diameter of the same disc when it is cold. Note that as the shrinkage is isotropic, the volumetric shrinkage is η^3.

non-Euclidean discs and tubes are presented in Fig. 7. These different plates show that one can indeed engineer plates with a prescribed metric, which can be elliptic ($\bar{K} > 0$), hyperbolic ($\bar{K} < 0$), or include different curvature profiles. The same principles are applicable in other topologies, such as tubes. This system allows for a quantitative study of the mechanics of NEP, as it provides an accurate and independent control over the relevant parameters of the system, such as thickness, radius and metric. For example, by a control of C(r) we construct *discs of constant Gaussian curvature* whose target metrics (with respect to the rescaled radial coordinate) are given by:

$$g = \begin{pmatrix} 1 & 0 \\ 0 & \frac{1}{\bar{K}}\sin^2\sqrt{\bar{K}}\rho \end{pmatrix}$$

For $\bar{K}>0$, and:

$$g = \begin{pmatrix} 1 & 0 \\ 0 & \frac{1}{-\bar{K}}\sin h^2\sqrt{-\bar{K}}\rho \end{pmatrix}$$

For $\bar{K}<0$.

Measurements of the buckled discs (see details in the next section) show that indeed on average the metric of the configurations is very close to that a surface of constant curvature (Fig. 8).

The usage of responsive gels has another advantage: the flat-to-curved transition is an induced reversible one. This allows the construction of responsive discs that can undergo an induced reversible shape transformation. They can, thus, turn into "soft machines" that utilize the new rich range of shape transformations found in non-Euclidean plates.

One can take a step forward and improve the control and the flexibility of target metric determination. This can be done by selective UV cross linking of the NIPA polymer. In this technique one needs to use a UV activated initiator for the cross linking reaction. Then, as in lithography, shine UV light on the polymer solution through a printed mask. This technique allows

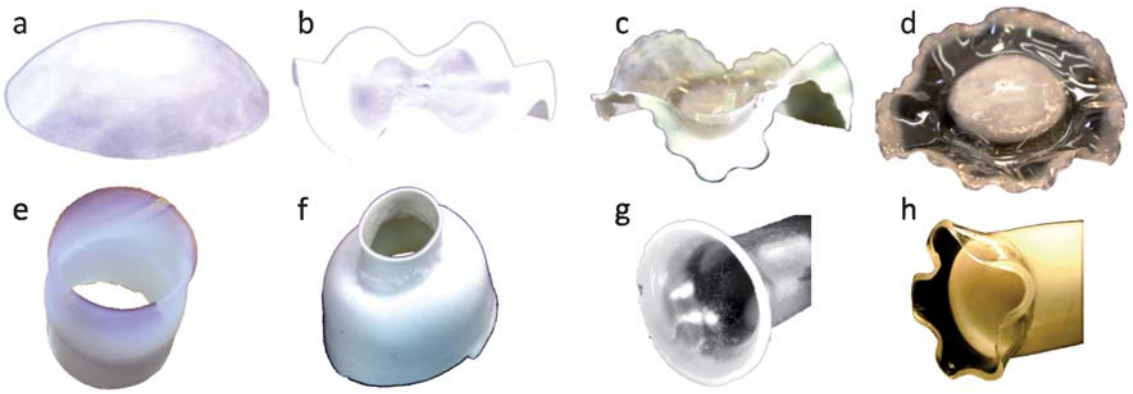

Fig. 7 Non-Euclidean plates and tubes made of NIPA gel. Examples of plates with $\bar{K} > 0$ (a), $\bar{K} < 0$ (b, c) and a disc that contains a central region of $\bar{K} > 0$ and an outer part of $\bar{K} < 0$ (d). (e)-(h) Non-Euclidean tubes. A tube with a metric similar to the one in Fig. 5 in its cold (e) and warm (f) states. Tubes with negative curvature bellow (g) and above (h) the "buckling-wrinkling" transition (see section 5.3).

"printing" a wide range of target metrics in a high spatial resolution. An example is presented in Fig. 9.

There are many other materials that can be used for the construction of NEP and responsive NEP. Materials such as electro active polymers[26] or nematic elastomers[27] seem to be excellent candidates for using the shaping principles, with responses in different time scales and environments.

Finally, we mention alteration of growth in plants as a way of constructing "biological NEP". Growth of tissue can be viewed as a process in which the target metric is constantly updated. It was shown that genetic manipulation,[28] as well as hormone treatment[29] can alter the growth distribution and cause a naturally flat leaf to become non-Euclidean. Similar effects often occur as a result of fungus attacks, when the leaf tissue grows without proper control (Fig. 10).

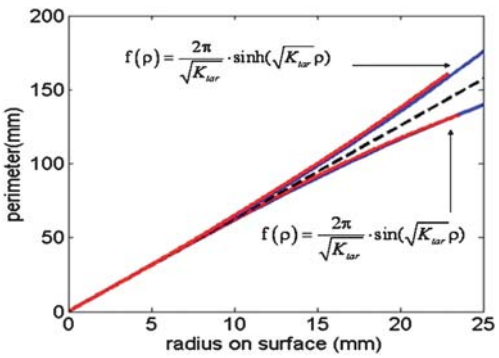

Fig. 8 Engineering discs with constant Gaussian curvature. The perimeter of a circle on a disc as a function of its radius (measured along the surface) for discs of positive (bottom) and negative (top) constant $|\bar{K}| = 0.0011$ mm^{-2}. The blue lines are the calculated curves (the relevant functions are indicated). The red lines are the data measured on the buckled discs. The dashed line indicates a flat disc: $f(\rho) = 2\pi\rho$.

5. Some results and interpretations

After reviewing the theoretical framework and experimental techniques, we review the main results in this new field.

5.1 Rectangle geometry

Experiments in torn plastic sheets

As described before, in a controlled experiment the target metric, imposed by the plastic flow around the tear tip, is very simple and highly symmetric: it determines negative target Gaussian curvature, which is a function only of the distance from the edge, y. Surprisingly, the configurations of the sheets consist of a

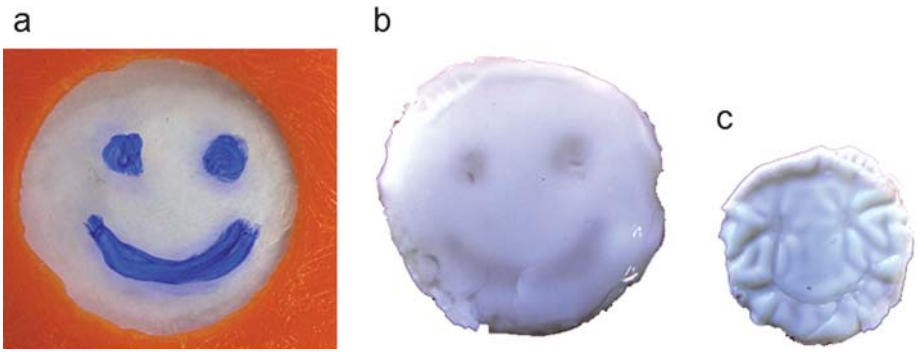

Fig. 9 "Lithography of curvature". (a) NIPA solution is inserted into simple mold with a "mask". Polymerization is controlled by a UV activated initiator (in this case Riboflavin), leading to the generation of a non-uniform gel disc (b). (c) The non-uniform shrinking properties of the gel turn into a non-Euclidean target metric. In this case the gradients in the metric are sharp, leading to wrinkling of the disc.

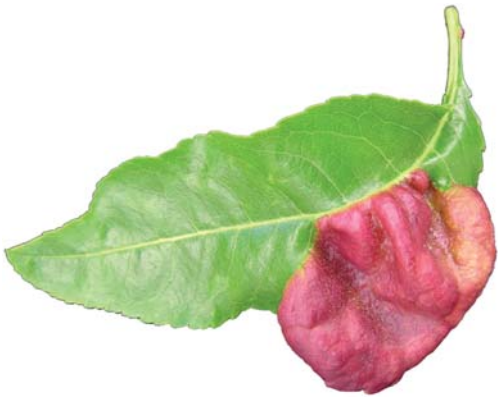

Fig. 10 An almond leaf which was attacked by *Taphrina Deformans*. The cells attacked by the fungus undergo rapid uncontrolled proliferation. As a result the leaf becomes non-Euclidean and undergoes buckling and wrinkling instabilities.

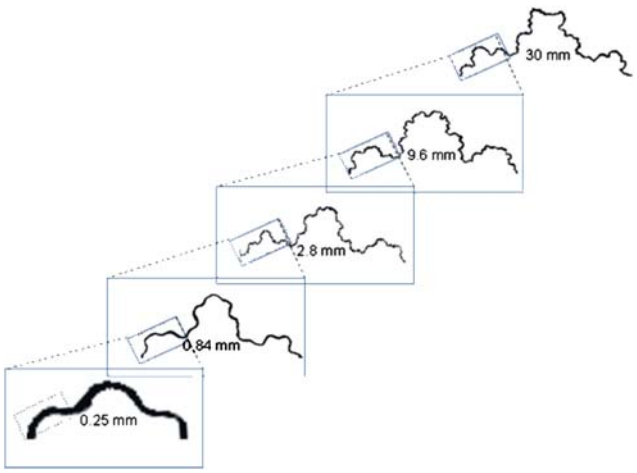

Fig. 11 Fractal scaling along the edge of torn plastic sheets: images of the edge of a 12 μm polyethylene sheet that was torn. The top figure shows the largest wavelength. Each subsequent image is obtained by zooming in a factor of 3.2 on the left "shoulder" of the former curve. The width of each wave is indicated. Data from ref. 18.

fractal-like hierarchical cascade of waves, where shorter waves are superimposed on longer ones[18] (Fig. 11). These experiments demonstrate how simple, symmetric metric can lead to multi-scale, ordered, 3D configurations. The origin of the observed fractal structures and their scaling was the subject of several works, that are described below, but is not yet fully understood.

Numerical simulations

Simulations of a rectangle plate with hyperbolic metric using both 3D discretized strip,[15] or modified 2D plate theory[16] obtained wavy and fractal-like stable configurations. In the 3D simulations the target metrics were introduced by specifying the local "rest length" of the springs that constructed the plate. The 2D modeling in ref. 16 involved linearization of the problem and the target metric was introduced by including a non-zero $\bar{K}$ in the stretching term. In this work the scaling of the shortest waves in the cascade was measured. The existence and scaling of the fractal pattern was explained in terms of minimum bending among stretch-free configurations. This proposed scenario is qualitatively similar to "ordinary buckling", presented in section 2.1.

An alternative view was suggested in ref. 19 where measurements of torn plastic sheets indicated that the wavelengths λ in the cascade has an explicit dependence on the thickness: $\lambda \propto t^{\frac{1}{3}} L^{\frac{2}{3}}$, where L is a length scale determined by $\bar{g}$. Such a scaling implies that there should be a *refinement* of the entire pattern as t decreases, *i.e.* a wrinkling-like mechanism. As explained in section 3.4, such a scaling would persist to increasingly smaller scales only if all zero stretching configurations have diverging bending content (as in the ruler-on-mattress example). Since we consider unconstrained sheets, this condition implies that for the relevant domain and metric there are no exact embeddings with "small enough" bending content. If there was such an embedding, there would be a thickness t^* bellow which the system would settle in its "vicinity" and smoothly converge to it, as required by the theorem in ref. 30. In this case λ should not have an explicit dependence on t, below t^*. Until now, experiments, as well as numerical works have not systematically studied the $t \to 0$ limit. It is not clear if the explicit dependence of λ on t is general, or if there is a cutoff thickness t^* below which the wrinkling-like behavior is replaced by "ordinary buckling".

5.2 Radial geometry

In the NIPA gel experiments, growth/shrinkage was tuned to be invariant parallel to the plate's margins, this time for circular discs. In these experiments discs with positive and negative Gaussian curvature were studied. A clear qualitative difference in their shaping was detected: the hyperbolic discs attained wavy configurations while discs with $\bar{K} > 0$ settled on a dome-like configurations (Fig. 12)[22]. It was shown that in both cases the perimeter of circles of radius ρ(r) on the buckled discs were very close to imposed perimeter, $2\pi r\eta(r)$. This measurement shows that the target metric is well approximated *on average* by the actual metric. In other words, in both cases, the metric of the selected configuration g is close to $\bar{g}$. However, measurements of the distribution of the Gaussian curvature on the discs showed qualitative differences between the hyperbolic and elliptic cases: for $\bar{K} > 0$ the measured local deviation of the Gaussian curvature K from $\bar{K}$ indicated concentration of small stretching deformations within boundary layers, as expected in "ordinary buckling"

Fig. 12 Discs of 0.6 mm initial thickness with constant positive (left) and negative (right) target Gaussian curvature $|\bar{K}| = 0.0011$ mm^{-2}, corresponding to the data presented in Fig. 8. For $\bar{K} > 0$ the disc attains a hemispheric configuration (with distinguishable boundary layer). For $\bar{K} < 0$ the configuration is wavy, breaking the axial symmetry. Measurements show that the number of waves depends on the thickness of the disc.

scenario and calculated in ref. 31. In contrast, for $\bar{K} < 0$ the measured Gaussian curvature strongly fluctuates around $\bar{K}$, indicating for possible periodic stress localization within the bulk of those configurations. Based on these observations it was argued that the two cases represent two different types of configurations: "ordinary buckling" in the case of $\bar{K} > 0$ and "wrinkling-like" in the case of $\bar{K} < 0$.

Recent theoretical study[31] of discs with $\bar{K} = \pm 1$ treated the two limiting thickness regimes. Thick discs contained a residual in-plane stress in a flat un-buckled state. Stability analysis of these plane stress solutions revealed a second order buckling transition at a critical thickness (Fig. 13 a). The analysis of the most unstable mode showed that the buckling of the $\bar{K} = -1$ disc must break the axial symmetry of the problem. The buckling of the $\bar{K} = 1$ disc preserves the axial symmetry. Within the thin disc limit, configurations are close to the bending minimizing isometric embedding of a disc with $\bar{K} = 1$—a spherical dome. The deviation from the isometric embedding was in the form of a *boundary layer* whose width scales like $t^{1/2}$ (Fig. 13 b). The effect of this boundary layer on the scaling of the bending and stretching energies was discussed.

A special case of circular flat discs in which radial sections of angle θ were inserted or removed was studied in ref. 32. The results were plates that were flat everywhere but contained a "defect" at their center. The defect contained Gaussian curvature in an amount that was set by the angle θ and could be positive (removing a section) or negative (inserting a section). Same intrinsic geometry could result from simple lateral anisotropic homogeneous growth of discs. The 3D equilibrium configurations of the discs were studied and were related to the shape evolution in growing biological systems. Such discs with high values of negative curvature defects were investigated.[33] A variety of 3D wavy configurations were found and the transition between them was studied.

In a recent work, wavy configurations observed in hyperbolic discs were studied.[34] Different approximations to the problem were used, in order to obtain solutions. In particular configurations of closed circular ribbons were studied. It was shown that the restriction of wavelengths due to periodicity requirements might lead to selected "resonances" in which the ribbon is embedded with distinctively low bending energy. Such conditions could affect wave selection in the full discs.

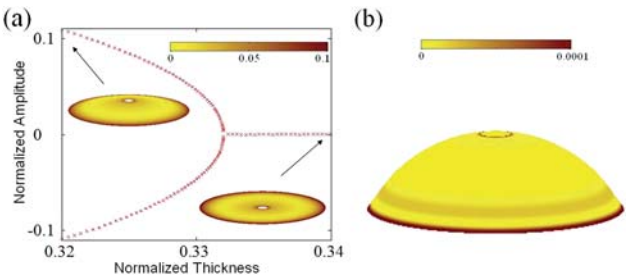

Fig. 13 (a) Buckling transition of a punctured disc ($0.1 < r < 1.1$) with $\bar{K} = 1$. The out of plane coordinate of the inner rim is plotted *versus* the thickness; both are normalized by $\sqrt{\bar{K}}$. The transition from the flat to the buckled configurations is second order and occurs at a normalized thickness of 0.3321. The branches of positive and negative amplitude are symmetric. They are selected by initial conditions. Inset: Configurations (mid surface) of discs of thickness 0.34 (right) and 0.32 (left) colored by their local stretching energy density per unit thickness. (b) Equilibrium configuration of a disc with the same intrinsic geometry as in (a) for a small but finite thickness (normalized thickness = 0.01). The disc is colored by the local stretching energy per unit thickness (note the three orders of magnitude difference from (a)). Most of the stretching energy is localized within a boundary layer. Results were obtained by numerically minimizing the elastic energy (eqn (4)) under the assumption of axial symmetry. The energy density is given in arbitrary units as in ref. 31, and the Poisson ratio $\upsilon = \frac{1}{3}$.

5.3 Non-Euclidean tubes

Non-Euclidean metric can be prescribed on other topologies, such as a tube. This is a good example showing how global limitations on the embedding "force" the physical system to undergo a mechanical instability and to switch from buckling-like to wrinkling-like configurations. Take a ring of cells and grow a "sleeve" from it by adding rings on top of it (Fig. 13 a). Let the number of cells in a ring grow exponentially with the index of the ring (the same body could be generated not by adding cells, but by taking a cylindrical sleeve and causing it to swell exponentially as in Fig. 7 g). What shape will this tube attain? We can find an embedding which keeps the axial symmetry and has low bending content. It will be in the form of a "trumpet". Indeed, the physical tube buckles into such axis-symmetric configuration (Fig. 7 g). As long as the funnel is "short" there is no problem (Fig. 14 a, b). However, if we let the funnel keep growing until its rim is horizontal we "hit a geometrical boundary". It is simply *the end of the axis-symmetric surface*. The growth law requires that the perimeter of the rim of radius r will be larger than $2\pi r$ (Fig. 14 c) and this is impossible in our Euclidean space. This global embedding issue is not of any "interest" for the cells that keep on growing exactly according to the same law. We see that if we want to avoid huge compression along the edge, something must happen. Indeed, experiments using NIPA gels (see Fig. 7 h), as well as numerical simulations[29] have shown that close to "geometrical boundary" the axis-symmetric funnel shape is replaced by a wavy tube shape that resembles the center part of a Daffodil (Fig. 14 d). This transition from a symmetric "featureless" buckling-like configuration to a wavy, wrinkling-like, one is driven solely by the limitations on possible embeddings of the relevant metric and topology in Euclidean space. A detailed study of this "trumpet" system can be found in ref. 11.

5.4 The embedding of hyperbolic metrics

As seen in the previous sections, the type of shaping mechanism ("ordinary" buckling or "wrinkling-like") of hyperbolic sheets (of negative Gaussian curvature) depends on the type of existing embeddings of hyperbolic metrics in Euclidean space. This mathematical problem of existence and smoothness of embeddings of 2D manifolds in 3D flat space was studied extensively, and was shown to be non trivial. The main challenge for a configuration is to handle the accelerating divergence of geodesics, or simply to "take care" of the rapid increase in the perimeter of a surface. Hilbert proved that there is no smooth embedding of the entire hyperbolic plane surface of ($K = -1$) in

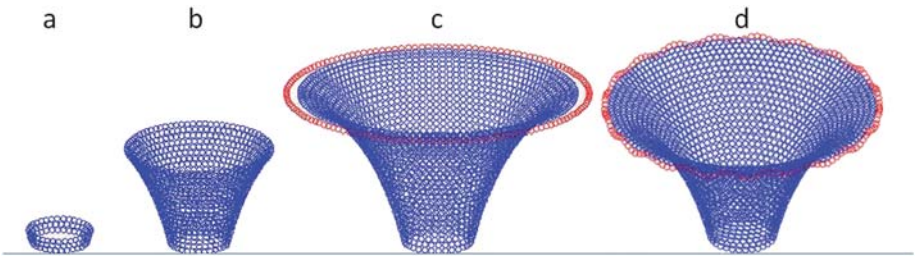

Fig. 14 Instability due to limitations on embedding. An illustration of a tube, which grows upwards by adding rows of cells. The number of cells in a ring increases exponentially upwards. As long as the tube is short (a, b) there exists an axi-symmetric embedding in the form of a "funnel". If the funnel keeps on growing, this shape is terminated when the rim of the funnel is horizontal. Beyond this point, an axi-symmetric configuration would require that a ring of radius r will have a perimeter larger than $2\pi r$ (c), which is impossible in our flat space. The sheet selects a different type of solution—a wavy one (d).

R^3 (ref. 35) and Efimov refined the theorem for non-constant Gaussian curvature (see ref. 36). Though these theorems show that hyperbolic metrics are "problematic", they do not have a dramatic effect on what we can say about elastic sheets of finite size. Poznyak and Shikin have constructed explicit embeddings with finite bending content for discs and strips of finite size.[37] These embeddings involve rolling of the plates and the bending content rapidly increases with the size of the disc. The relevance of these embeddings to the mechanical problem was not fully studied. However, until now such configurations were not observed in experiments or simulations, as energy minima. It is likely that a progress in the study of the embedding of finite size sheets will affect our understanding of shaping mechanisms of NEP.

6. Characteristics and applicative potential

We are now ready to look at some characteristics of NEP as a shaping mechanism, having in mind their applicative potential.

• As demonstrated above, the mechanics of non-Euclidean plates converts 2D information—the target metric—into 3D configurations. This is an efficient way of shaping 3D objects. In some cases the 3D configurations consist of multi-scale, or small scale structure. This happens when the dominant behavior is of wrinkling-type. As presented, such a behavior can appear even when the target metric is highly symmetric and "featureless". In such cases one gets "for free" complex 3D configurations whose manufacturing by other techniques could be difficult and expensive.

• Some of the multi-scale configurations that are formed are convolved and closed on themselves. It is difficult to produce such structures using other shaping techniques, such as machining, casting or pressing.

• Another important property is the unusually *wide range of possible shapes* that can be attained by a single body. The only prescribed quantity in NEP is the target metric, *not any configuration*. In general there are many embeddings for a metric, so a plate can "investigate" a wide range of configurations that can be very different from each other. Thus, small changes in $\bar{g}$ can cause *dramatic shape changes* in the body. An example is the growing trumpet (section 5.3), where a "symmetric-to-wavy transition" was demonstrated. This property is in contrast with the fixed accessible configurations in other shaping methods such as shape memory materials. It could be of importance for different applications.

• When constructed from responsive materials NEP undergo reversible shape changes, turning into flexible "*soft machines*". This property can be useful for different bio-mechanical applications.

These are probably just part of the unique, useful properties of non-Euclidean plates. It is likely that some other characteristics will be reviled in the future.

7. Open questions

In this last section we try to point out some of the main challenges and open questions in this new field.

• As could be understood from the previous sections the origin and scaling of the fractal structures that appear in hyperbolic plates is not understood yet. It seems like such plates shape themselves *via* wrinkling-like instability. However the geometrical origin of this behavior is not well understood. There are several results regarding the embedding of finite discs, that seems to exclude the wrinkling-like scenario. There is still no coherent picture that connects these results with experimental observations.

• A technical challenge would be to build NEP from responsive materials other than NIPA. As any elastic theory, the theory of NEP is not limited to specific materials or specific scales. It is likely that NEP can be built from materials such as nematic ellastomers, electroactive polymers or different alloys. This would increase the applicative potential of NEP.

• Another interesting direction is the extension to "frustrated shells"—bodies with non-vanishing first and second fundamental forms that are not necessarily compatible with each other. Though the theoretical framework was developed,[38] only simple cases were studied, and it would be interesting to see what will be the properties of such bodies. It is likely that some structures of this type undergo dynamic shape transition, like the snapping of the venus flytrap.[39]

• An important subject, which was not addressed in this review, is the relevance of NEP mechanics to the development of living tissue. There are examples that show how 3D configurations develop in growing bodies, such as leaves[40] and indications for possible role of mechanics in development.[41] There is still a need for quantitative study in this field.

These are just few of the potential directions. The readers are likely to develop their own view and taste and identify interesting problems in this fresh field of research.

Note added after first publication

This article replaces the version published on 8th October 2010, which contained errors in the equations on page 7.

Acknowledgements

We thank G. Cohen for assisting in writing this paper. This work was supported by the ERC "SoftGrowth" project.

References

1 C. C. Wang, On the Geometric Structures of Simple Bodies, a Mathematical Foundation for the Theory of Continuous Distributions of Dislocations, *Arch. Ration. Mech. Anal.*, 1967, **27**, 33–94.
2 A. Hoger, Residual stress in an elastic body: a theory for small strains and arbitrary rotations, *J. Elasticity*, 1993, **31**(1), 1–24.
3 E. K. Rodriguez, A. Hoger and A. D. McCulloch, Stress-dependent finite growth in soft elastic tissues, *J. Biomech.*, 1994, **27**(4), 455–467.
4 A. Goriely and M. Ben Amar, Differential growth and instability in elastic shells, *Physical Review Letters*, 2005, (19), 94.
5 F. John, Estimates for the derivatives of the stresses in a thin shell and interior shell equations, *Commun. Pure Appl. Math.*, 1965, **18**(1–2), 235–267.
6 L. D. Landau and E. M. Lifshitz, *Teory of Elasticity*, 3rd edn, 1986,Oxford, Pergamon Press.
7 E. Cerda and L. Mahadevan, Geometry and physics of wrinkling, *Phys. Rev. Lett.*, 2003, **90**(7), 074302.
8 E. Cerda, K. Ravi-Chandar and L. Mahadevan, Thin films - Wrinkling of an elastic sheet under tension, *Nature*, 2002, **419**(6907), 579–580.
9 N. Bowden, *et al.*, Spontaneous formation of ordered structures in thin films of metals supported on an elastomeric polymer, *Nature*, 1998, **393**(6681), 146–149.
10 R. Huang and Z. Suo, Wrinkling of a compressed elastic film on a viscous layer, *J. Appl. Phys.*, 2002, **91**(3), 1135–1142.
11 M. Marder and N. Papanicolaou, Geometry and elasticity of strips and flowers, *J. Stat. Phys.*, 2006, **125**, 1069–1096.
12 B. O'Neill, *Elementary Differential Geometry*, 2nd edn, 1997,New York, Academic Press.
13 E. Efrati, E. Sharon and R. Kupferman, Elastic theory of unconstrained non-Euclidean plates, *J. Mech. Phys. Solids*, 2009, **57**(4), 762–775.
14 W. T. Koiter, On the foundations of the linear theory of thin elastic shells. I, II. Koninklijke Nederlandse Akademie van Wetenschappen, *Proceedings. Series B. Physical Sciences*, 1970, **73**, 183–195.
15 M. Marder, *et al.*, Theory of edges of leaves, *Europhys. Lett.*, 2003, **62**(4), 498–504.
16 B. Audoly and A. Boudaoud, Self-similar structures near boundaries in strained systems, *Phys. Rev. Lett.*, 2003, **91**(8), 086105.
17 J. Dervaux, P. Ciarletta and M. Ben Amar, Morphogenesis of thin hyperelastic plates: A constitutive theory of biological growth in the Föppl-von Kármán limit, *J. Mech. Phys. Solids*, 2009, **57**(3), 458–471.
18 E. Sharon, *et al.*, Mechanics: Buckling cascades in free sheets, *Nature*, 2002, **419**(6907), 579–579.
19 E. Sharon, B. Roman and H. L. Swinney, Geometrically driven wrinkling observed in free plastic sheets and leaves, *Phys. Rev. E: Stat., Nonlinear, Soft Matter Phys.*, 2007, **75**(4), 046211.
20 D. W. Henderson and D. Taimina, Crocheting the hyperbolic plane, *The Mathematical Intelligencer*, 2001, **23**, 17–28.
21 D. Taimina, *Crocheting Adventures with Hyperbolic Planes*. 2009, Wellesley, A K Peters.
22 Y. Klein, E. Efrati and E. Sharon, Shaping of elastic sheets by prescription of non-Euclidean metrics, *Science*, 2007, **315**(5815), 1116–1120.
23 E. Efrati, *et al.*, Spontaneous buckling of elastic sheets with a prescribed non-Euclidean metric, *Phys. D*, 2007, **235**, 29–32.
24 T. Tanaka, Collapse of Gels and Critical Endpoint, *Phys. Rev. Lett.*, 1978, **40**(12), 820–823.
25 O. E. Philippova, *et al.*, pH-Responsive Gels of Hydrophobically Modified Poly(acrylic acid), *Macromolecules*, 1997, **30**(26), 8278–8285.
26 Y. Bar-Cohen, Electroactive polymers as artificial muscles: A review, *J. Spacecr. Rockets*, 2002, **39**(6), 822–827.
27 D. L. Thomsen, *et al.*, Liquid crystal elastomers with mechanical properties of a muscle, *Macromolecules*, 2001, **34**(17), 5868–5875.
28 U. Nath, *et al.*, Genetic control of surface curvature, *Science*, 2003, **299**(5611), 1404–1407.
29 E. Sharon, M. Marder and H. L. Swinney, Leaves, flowers and garbage bags: Making waves, *American Scientist*, 2004, **92**(3), 254–261.
30 M. Lewicka and M. R. Pakzad, Scaling laws for non-Euclidean plates and the W2;2 isometric immersions of Riemannian metrics, *Preprint*, 2009.
31 E. Efrati, E. Sharon and R. Kupferman, Buckling transition and boundary layer in non-Euclidean plates, *Phys. Rev. E: Stat., Nonlinear, Soft Matter Phys.*, 2009, **80**(1), 016602.
32 J. Dervaux and M. Ben Amar, Morphogenesis of growing soft tissues, *Phys. Rev. Lett.*, 2008, **101**(6), 068101.
33 M. M. Muller, M. Ben Amar and J. Guven, Conical Defects in Growing Sheets, *Phys. Rev. Lett.*, 2008, **101**(15), 156104–4.
34 C. D. Santangelo, Buckling thin disks and ribbons with non-Euclidean metrics, *Europhys. Lett.*, 2009, **86**(3), 34003.
35 D. Hilbert, *Trans. Am. Math. Soc.*, 1901, **2**, 87.
36 T. K. Milnor, Efimov's theorem about complete immersed surfaces of negative curvature*1, *Advances in Mathematics*, 1972, **8**(3), 474–543.
37 E. Poznyak and E. Shikin, Small parameter in the theory of isometric imbeddings for two-dimensional Riemannian manifolds into euclidean spaces, *Journal of Mathematical Sciences*, 1995, **74**(3), 1078–1116.
38 E. Efrati, E. Sharon and R. Kupferman, *Non-Euclidean Plates and Shells*, to be published, 2010, see http://www.ma.huji.ac.il/~razk/Publications/short.html.
39 Y. Forterre, *et al.*, How the Venus flytrap snaps, *Nature*, 2005, **433**(7024), 421–425.
40 E. Coen, *et al.*, The genetics of geometry, *Proc. Natl. Acad. Sci. U. S. A.*, 2004, **101**(14), 4728–4735.
41 O. Hamant, *et al.*, Developmental Patterning by Mechanical Signals in Arabidopsis, *Science*, 2008, **322**(5908), 1650–1655.

